International Journal of Multiphase Flow 35 (2009) 163–170

Contents lists available at ScienceDirect

International Journal of Multiphase Flow

journal homepage: www.elsevier.com/locate/ijmulflow

On the particle inertia-free collision with a partially contaminated spherical bubble

Dominique Legendre [a,b,*], Vincent Sarrot [a,b,c,d,e], Pascal Guiraud [c,d,e]

[a] Université de Toulouse; INPT, UPS; IMFT (Institut de Mécanique des Fluides de Toulouse); Allée Camille Soula, F-31400 Toulouse, France
[b] CNRS; IMFT; F-31400 Toulouse, France
[c] Université de Toulouse; INSA,UPS,INP; LISBP, 135 Avenue de Rangueil, F-31077 Toulouse, France
[d] INRA, UMR792 Ingénierie des Systèmes Biologiques et des Procédés, F-31400 Toulouse, France
[e] CNRS, UMR5504, F-31400 Toulouse, France

ARTICLE INFO

Article history:
Received 15 March 2008
Received in revised form 4 October 2008
Accepted 5 October 2008
Available online 17 October 2008

ABSTRACT

The collision between a contaminated spherical bubble and fine particles in suspension is considered for $r_p/r_b \ll 1$ (r_p being the radius of the particles in suspension and r_b the radius of the bubble). The collision probability or efficiency is defined as the number of particles colliding the bubble surface to the number of particles initially present in the volume swept out by the bubble. In this note we show that the collision probability can be expressed as $P_c(r_p/r_b,Re) = g(r_p/r_b)f(Re)$ for both mobile and immobile interfaces. For partially contaminated bubbles a linear or quadratic dependency in r_p/r_b is found depending on the level of contamination and the value of r_p/r_b. These behaviors are given by the flux of particles near the surface which is controlled by the tangential velocity for mobile interfaces and by the velocity gradient for immobile interfaces. The threshold value $(r_p/r_b)_{th}$ between the r_p/r_b and $(r_p/r_b)^2$ evolution is shown to vary as $\sin^{n(Re)}(\theta_{clean}/n(Re))\sin(3\theta_{clean}/4)$, θ_{clean} being the angle describing the front clean part of the bubble and $n(Re)$ varying from $n = 2$ to $n = 1$ from small to large Reynolds number.

1. Introduction

The collision between bubbles and particles in suspension occurs in many applied situations, like water treatment, mining exploitation, liquid metal purification, chemical reactors and dynamics of air-sea exchange. In most of these situations bubbles capture particles in suspension and transport them at a free surface. The mechanisms of particle-bubble capture combine the dynamics of collision with the interfacial forces between the bubble surface and the particles. An overall capture probability (or capture efficiency) is usually defined as the ratio between the number of particles captured by a bubble and the number of particles located in the volume swept out by the bubble. This overall probability can be decomposed as the product of three contributions (Schulze, 1989; Dai et al., 2000; Ralston et al., 2002; Nguyen and Schulze, 2004): the efficiency of collisions P_c between bubbles and particles that can be considered as a pure hydrodynamic mechanism, the attachment efficiency and the particle-bubble aggregate stability efficiency. Experimentally it is not easy to evaluate the contribution of each sub-probability since one only access to the total number of particles captured by several bubbles. The analyze of the results and the comparison with theoretical models are performed with the assumption of unity attachment efficiency and zero detachment efficiency. The hydrophobic, Van der Walls and electrostatic forces are known to play a significant role during the attachment and on the stability of the particle-bubble aggregate. As mention in Nguyen and Schulze (2004), the contamination of the bubble interface is one possible reason explaining the difference between experiments and theoretical predictions. The effect of the interface mobility on the collision probability is also qualitatively discussed in Dukhin et al. (1995). In the previous studies dealing with capture efficiency, the effect of the interface contamination on the collision efficiency has only been analyzed by considering a fully mobile or immobile bubble surface. The contamination is generated by the presence of impurities or surfactants and also by the accumulation of captured particles in suspension. The contamination of the bubble interface is well known to modify the bubble terminal velocity (Clift et al., 1978). In presence of surfactant molecules or impurities, the rising velocity is observed to range between the velocity of a clean bubble and the velocity of a bubble with a fully immobile interface. The difference between these two velocities can be significant. For example, considering a 1 mm bubble in water under normal conditions, the rising velocity is around 25 cm/s for a clean bubble while it is 11 cm/s for a fully contaminated bubble. In most of the practical situations, bubble interfaces are partially contaminated. Thanks to the analytical solution in Stokes flow obtained by Sadhal and Johnson (1983) and numerical simulations (RBel and Duineveld, 1996; McLaughlin, 1996; Cuenot et al., 1997) for low to moderate Reynolds numbers, relations between the drag force and the level of contamination have been obtained. The inspection of such numerical simulations clearly show that the flow field around a bubble is

* Corresponding author. Address: Institut de Mécanique des Fluides - UMR CNRS 5502, Allée du Professeur Camille Soula, 31400 Toulouse, France.
E-mail address: legendre@imfr.fr (D. Legendre).

0301-9322/$ - see front matter © 2008 Elsevier Ltd. All rights reserved.
doi:10.1016/j.ijmultiphaseflow.2008.10.002

strongly influenced by the level of contamination resulting in a significant effect on the behavior of the probability of collision (Sarrot et al., 2005). In this paper we focus on the effect of the level of contamination on the collision probability between a spherical bubble and fine particles in suspension. We consider situations from fully mobile to fully immobile interface. The objective is to give a pertinent modeling of the effect of the partial contamination of the bubble interface based on direct numerical simulations and hydrodynamical arguments.

2. Statement of the problem

The radii of the bubble and the particles in suspension are denoted r_b and r_p, respectively. The liquid velocity is considered steady and uniform at the bubble scale. U_b denotes the relative velocity of the bubble and $Re = 2r_bU_b\rho/\mu$ its Reynolds number, ρ and μ being the density and the viscosity of the surrounding liquid. We consider fine particles of density ρ_p so that their Stokes number $St = 2\rho_p r_p^2 U_b/9\ \mu r_b$ and the ratio of their velocity V_p to the bubble velocity U_b are both much smaller than unity. Typically, if we consider a bubble rising in a suspension of particles, the ratio between the sedimenting particle velocity V_S and the rising bubble velocity U_b scales as $V_S/U_b \sim (r_p/r_b)^2$ so that in the limit $r_p/r_b \to 0$ the velocity perturbation imposed by the sedimentation of each particle is small compared to the velocity field imposed by the rising bubble. For example, considering a $r_b = 0.5$ mm air bubble in motion in water which contains particles of radius $r_p = 5\ \mu$m and density $\rho_p = 2500\ \text{kg/m}^3$, the Stokes number is $St \sim 0.005$ and the velocity ratio is $V_S/U_b \sim 0.001$. Considering the limit $St \to 0$ and $r_p/r_b \to 0$, a particle basically follows the streamlines of the flow imposed by the bubble motion. Under these conditions the probability of collision between a bubble and a particle is only dependent on the ratio r_p/r_b, the bubble Reynolds number Re and the mobility of the surface (level of contamination).

We denote Ψ_{col} the maximum value of the stream function at the distance r_p from the bubble surface and θ_{col} the corresponding angle defined from the front stagnation point (Fig. 1a). A particle of radius r_p collides with the bubble surface if it follows a streamline passing between the bubble surface and the limit streamline Ψ_{col}. We define the probability (or efficiency) of collision as the ratio between the number of particles which collide with the bubble surface to the number of particles contained in the volume swept out by the bubble. For a free rectilinear rising bubble, this volume is a cylinder of section πr_b^2. If the concentration of particles is uniform, the flux of captured particles is directly proportional to the flow rate Φ_{col} and the probability of collision can be written as:

$$P_c\left(\frac{r_p}{r_b}, Re\right) = \frac{\Phi_{col}}{\pi r_b^2 U_b} = \frac{2\Psi_{col}}{r_b^2 U_b} \tag{1}$$

In this note, we propose to evaluate the flux of particles which collide with the surface by calculating the flow rate Φ_{col} between the streamline Ψ_{col} and the bubble surface at the angular position $\theta = \theta_{col}$:

$$\Phi_{col} = \int_0^{r_p} u(y, \theta_{col}) 2\pi (r_b + y) \sin\theta_{col} dy \tag{2}$$

where $y = r - r_b$ is the radial distance from the surface. The flow rate is calculated by considering a Taylor expansion of the tangential velocity $u(y,\theta_{col}) = U_\Gamma + y(\partial u/\partial\ y)_\Gamma + O(y^2)$ where U_Γ and $(\partial u/\ \partial y)_\Gamma$ are the tangential velocity and the velocity gradient at the surface, respectively. Combining this relation with (2), the probability of collision writes:

$$P_c\left(\frac{r_p}{r_b}, Re\right) = 2\frac{r_p}{r_b}\frac{U_\Gamma}{U_b}\sin\theta_{col} + \frac{r_p^2}{r_b^2}\left[\frac{U_\Gamma}{U_b} + \frac{r_b}{U_b}\left(\frac{\partial u}{\partial y}\right)_\Gamma\right]\sin\theta_{col} + O\left(\frac{r_p^3}{r_b^3}\right) \tag{3}$$

Note that this relation is valid whatever the value of Re and the mobility of the interface in the limit $r_p \ll r_b$. The position $\theta = \theta_{col}$ where the streamlines get closer to the interface and the corresponding values of U_Γ and $(\partial u/\partial y)_\Gamma$ only depend on the bubble dynamics i.e. they are only function of Re.

For a clean spherical bubble, the slip condition at the surface results in a tangential velocity of order U_b. The corresponding zero shear stress condition $\partial u/\partial y - u/r_b = 0$ at the bubble surface gives a flow rate directly proportional to U_Γ and $\sin\theta_{col}$ and the probability of collision is:

$$P_c\left(\frac{r_p}{r_b}, Re\right) = \frac{r_p}{r_b}\left(1 + \frac{r_p}{r_b}\right) f^I(Re) \quad \text{with} \quad f^I(Re) = 2\frac{U_\Gamma}{U_b}\sin\theta_{col} \tag{4}$$

Under Stokes conditions ($Re = 0$), the analytical solution gives $U_\Gamma = U_b/2$ and $\theta_{col} = \pi/2$ by symmetry. Consequently, $f^I(Re \to 0) = 1$ and relation (3) gives $P_c(Re \to 0) = r_p/r_b(1 + r_p/r_b)$. At high Reynolds number the flow around a clean bubble is known to be asymptotically potential (Moore, 1963). For a potential flow $\theta_{col} = \pi/2$ by symmetry and $U_\Gamma = 3U_b/2$ so that $f^I(Re \to \infty) = 3$ and relation (3) gives $P_c(Re \to \infty) = 3r_p/r_b(1 + r_p/r_b)$ where the first term $3r_p/r_b$ is the famous result of Sutherland (1948). For intermediate Reynolds numbers, the angle of collision has been determined using direct numerical simulations and was found to be close to $\theta_{col} \sim \pi/2$, the corresponding correction in (4) being less than 1.5% (Nguyen, 1998, Sarrot et al., 2005, Nguyen et al., 1998). Consequently, considering expression (4), the expression of f^I is given by the evolution of the tangential velocity at the bubble surface. This can be found in Legendre (2007) where the tangential velocity is shown to be directly link to the drag coefficient so that $f^I(Re) = (16 + 3.315\ Re^{1/2} + 3Re)/(16 + 3.315Re^{1/2} + Re)$. The comparison with previous correlations show that the function $P_c = r_p/r_b(1 + 2/(1 + (0.37/Re)^{0.85}))$ given by Weber and Paddock (1983) and $P_c = r_p/r_b(X + Y\cos\theta_{col})(1 - \cos^2\theta_{col})$ given by Nguyen (1998) with $X = 1 + 0.0637Re/(1 + 0.0438Re^{0.976})$, $Y = 1 + 0.0537Re/(1 + 0.0318Re^{1.308})$ and $\cos\theta_{col} = ((X^2 + 3Y^2)^{1/2} - X)/3Y$ give comparable evolutions for the function f^I.

At the surface of a solid sphere ($U_\Gamma = 0$), the flow rate is $\Phi_{col} = \pi r_b \sin\theta_{col} r_p^2\ (\partial u/\partial\ y)_\Gamma$ and the probability of collision is directly proportional to the velocity gradient at the surface:

$$P_c\left(\frac{r_p}{r_b}, Re\right) = \left(\frac{r_p}{r_b}\right)^2 f^{II}(Re) \quad \text{with} \quad f^{II}(Re) = \frac{r_b}{U_b}\left(\frac{\partial u}{\partial y}\right)_\Gamma \sin\theta_{col} \tag{5}$$

Considering the Stokes solution $(\partial u/\partial y)_\Gamma = 3\ U_b/2r_b$ from which we deduce $f^{II}(Re = 0) = 3/2$, relation (3) gives $P_c(Re = 0) = 3r_p^2/2r_b^2$ (Gaudin, 1957). At moderate Reynolds to high Reynolds numbers, θ_{col} decreases due to the increase of the recirculation zone with Re. The corresponding evolution can be simply modeled by $\sin\theta_{col} \sim Re^{-0.03}$ for $10 < Re < 250$, $\sin\theta_{col}$ slightly depending on r_p/r_b (Sarrot, 2006). Due to the evolution of the boundary layer thickness $\delta/r_b \sim Re^{-1/2}$ at a solid sphere surface, the velocity gradient can be estimated by $(\partial u/\partial y)_\Gamma \sim U_b/\delta \sim Re^{1/2}U_b/\ r_b$ which gives the asymptotic limit $f^{II}(Re \to \infty\ ) \propto Re^{1/2}$. Combining this relation with $\sin\theta_{col}\ \sim Re^{-0.03}$, the collision probability is shown to evolve as $P_c(Re \to \infty) \propto (r_p/r_b)^2 Re^{0.47}$ (Sarrot, 2006) in agreement with the relation $P_c = (3/2)\ (r_p/r_b)^2(1 + (3/16)Re/(1 + 0.249Re^{0.56}))$ given $P_c \propto 1.13\ Re^{0.44}$ in the limit $Re_b \to \infty$ (Weber and Paddock, 1983). Note that the behavior $P_c \propto Re^{2/3}$ proposed by Sarrot et al. (2005) and $P_c \propto Re^{0.72}$ given by Yoon and Lutrell (1989) are not in agreement with the hydrodynamic justification given in this note.

3. Collision with a partially contaminated bubble

Depending on the concentration of contaminant in the liquid, a bubble interface can be totally or partially contaminated. The distribution of contaminant on the interface results from the equilibrium between the adsorption and desorption at the interface, and

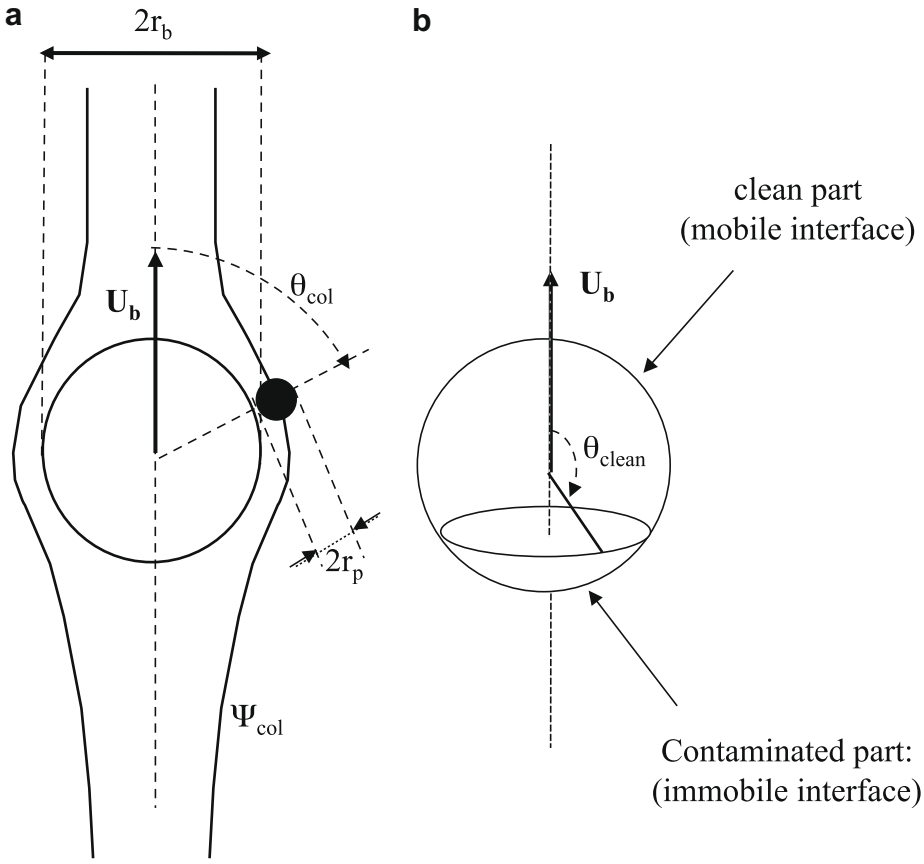

Fig. 1. (a) Definition of the parameters and the limit streamline Ψ_{col}. (b) Stagnant cap model used to describe a partially contaminated bubble.

the tangential advection and diffusion along the interface. When the tangential advection dominates the diffusion so that the surfactants accumulate at the rear part of the bubble, the interface contamination can be modeled with a good accuracy with the stagnant cap model (Dukhin et al., 1995; RBel and Duineveld, 1996; McLaughlin, 1996; Cuenot et al., 1997). This description of the contamination consists in separating the interface into two parts. The front part $0° < \theta < \theta_{clean}$ is free of any surfactants and the interface is mobile due to the zero-shear stress condition while the rear part of the bubble $\theta_{clean} < \theta < 180°$ is saturated on surfactants and the resulting immobile interface obeys a non-slip condition (Fig. 1b). Using this description of the surface, the numerical simulations of Sarrot et al. (2005) show that two different behaviors are observed for the probability of collision depending on the level of contamination of the interface. For $\theta_{clean} > 90°$ the collision occurs on the mobile part of the bubble and the probability of collision always follows a linear evolution in r_p/r_b. For $\theta_{clean} < 90°$, a r_p/r_b or $(r_p/r_b)^2$ evolution is observed depending on the values of r_p/r_b and Re. The probability of collision is found to change from the linear dependency to the quadratic evolution at a threshold value $(r_p/r_b)_{th}$ depending mainly on the level of mobility of the interface.

The existence of a threshold radius ratio $(r_p/r_b)_{th}$ is the direct consequence of the shape of the streamlines around a contaminated bubble. As illustrated by the drawing reported in Fig. 2, a streamline passing in the vicinity of the surface of the bubble can present in some particular conditions two local minimum positions. The first one, at the radial distance r_1 from the surface, is located on the front clean part of the bubble where the tangential velocity is maximum between its zero values at $\theta = 0$ and $\theta = \theta_{clean}$. At $\theta = \theta_{clean}$ due to the change of surface mobility, the non-slip condition induces a sharp reduction of the flow rate in the vicinity of the bubble and the streamlines are strongly deflected. If $\theta_{clean} < \pi/2$ the flow rate continues to increase in the vicinity of the bubble due to continuity and the streamlines can get closer to the surface and reach a second local minimum position at a radial distance r_2 from the surface corresponding to a local maximum of the velocity gradient. This second local minimum position is observed if the angle θ_{clean} is less than a critical value $\theta_{th}(Re)$ depending on the Reynolds number. The values of $\theta_{th}(Re)$ are reported in Table 1. $\theta_{th}(Re)$ is found to reach asymptotically two constant values, around 60° for low Reynolds number and close to 33° for large Reynolds number. The evolution of θ_{th} is found to be fitted with an accuracy less than 3% to the following correlation:

$$\theta_{th} = 33^\circ \frac{Re + 4.4}{Re + 2.5} \tag{6}$$

Depending on the comparison between the two local minimum distances r_1 and r_2, the collision is controlled by the clean part or by the contaminated part of the bubble. If $r_p = r_1 < r_2$, the probability of collision of particles of radius r_p is controlled by the clean part and evolves as r_p/r_b. If $r_p = r_2 < r_1$, the flux of particle colliding the surface is given by the flow near the non-mobile part and the probability of collision evolves as $(r_p/r_b)^2$. Consequently no progressive transition is observed between the linear and the quadratic evolution. The transition between the two regimes is observed when the limit streamline Ψ_{col} satisfies $r_1 = r_p = r_2$ which is observed when the flow rates on the clean and the contaminated parts are equal.

Fig. 3 reports the numerical values of $(r_p/r_b)_{th}$ obtained by Sarrot et al. (2005) for different Reynolds numbers. Some additional simulations have been performed in this study to cover a larger range of Reynolds number and a larger range of level of contamination. At first order a general evolution is observed. The values of $\theta_{th}(Re)$ are also reported in Fig. 3 using vertical dashed lines. For each value of Re two regions can be clearly defined. In the region above the

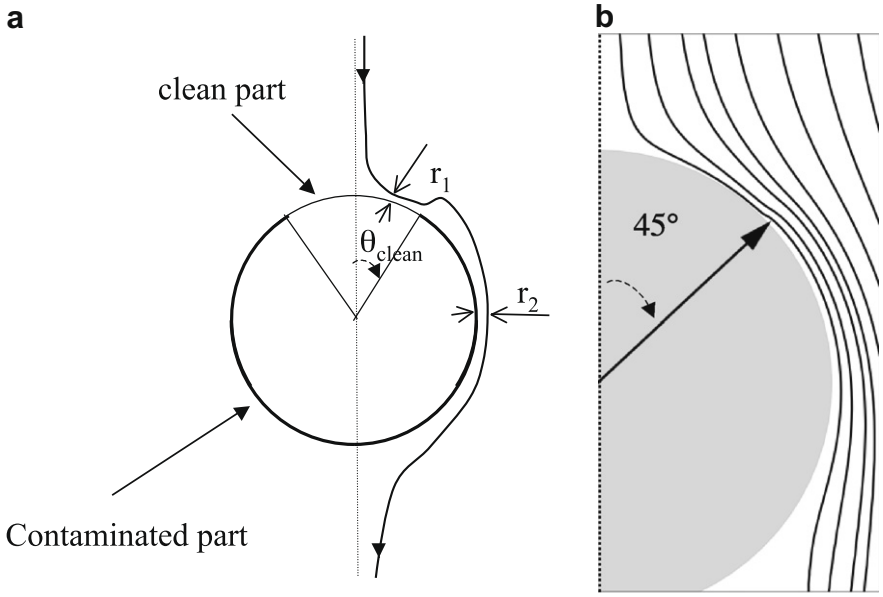

Fig. 2. Shape of the streamlines for a contaminated bubble for $0 < \theta_{clean} < \theta_{th}$. (a) Definition of the two local minimum distances r_1 and r_2. (b) Numerical simulation of the streamlines for $\theta_{clean} = 45^o$ and $Re = 100$ showing an example of the two local minimum distances. Here $r_1 < r_2$.

Table 1
Value of the maximum angle of contamination $\theta_{th}(Re)$ for the presence of two local minimum positions of the streamlines near the bubble surface.

Re	0.1	1	10	100	250
θ_{th}	56.7°	49.5°	38.7°	33°	33°

curve and delimited by the vertical dashed line $\theta_{th}(Re)$, the probability of collision is controlled by the contaminated part of the surface and the evolution is quadratic ($P_c \propto r_p^2/r_b^2$) while in the rest of the domain (r_p/r_b,θ_{clean}) the evolution is linear ($P_c \propto r_p/r_b$).

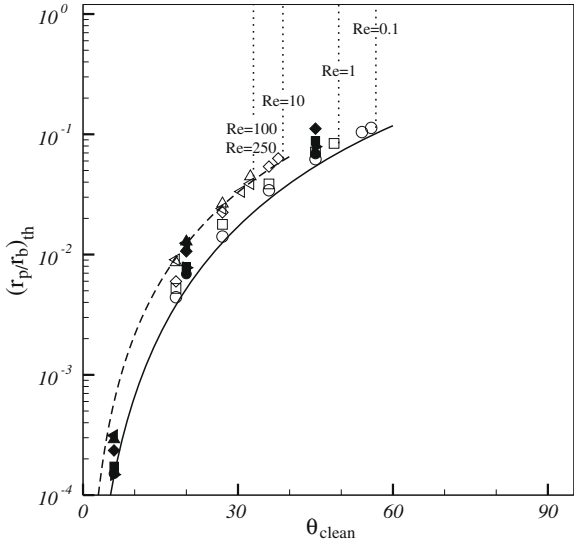

Fig. 3. Evolution of $(r_p/r_b)_{th}$ versus θ_{clean}. Filled symbols: Sarrot et al. (2005), empty symbols: this study. ○ $Re = 0.1$, □ $Re = 1$, ◇ $Re = 10$, △ $Re = 100$, ◁ $Re = 250$. — relation (13) for $Re = 0$, - - - relation (13) for $Re = 20$. Above the curve $P_c \propto r_p^2/r_b^2$, under the curve $P_c \propto r_p/r_b$ and the separation between the two regions is completely defined by the vertical dashed lines indicating the value of $\theta_{th}(Re)$ given in Table 1.

4. Probability of collision

4.1. Collision controlled by the clean part of the surface

According to relation (3), the flow rate on the clean part is controlled by the evolution of the tangential velocity at the surface and is given by its maximum value. The tangential velocity normalized by U_b is plotted in Fig. 4 versus θ for different levels of contamination and for two Reynolds numbers $Re = 1$ and $Re = 100$. As shown in this figure, the maximum value of the tangential velocity is observed at the angle $\theta_{col} < \theta_{clean}$ and its magnitude is found to be significantly less than the tangential velocity of a clean bubble at the angular position $\theta = \theta_{col}$.

The maximum tangential velocity $U_\Gamma(\theta_{clean})$ normalized by U_b is reported in Fig. 5 versus θ_{clean}. This figure shows that $U_\Gamma(\theta_{clean})$ evolves between two limit curves. In the Stokes limit ($Re \to 0$) one has $U_\Gamma^0(\theta_{clean}) = 1/2\sin^2(\theta_{clean}/2)$. In the limit of perfect fluid ($Re \to \infty$), U_Γ^∞ is given by the potential solution $U_\Gamma^\infty(\theta_{clean}) = 3/2\sin(\theta_{clean})$ for $\theta_{clean} \leqslant \pi/2$ and $U_\Gamma^\infty(\theta_{clean}) = 3/2$ for $\theta_{clean} \geqslant \pi/2$. This maximum value is obviously located at the angle $\theta_{col}^\infty = \theta_{clean}$ if $\theta_{clean} \leqslant \pi/2$ and at the angle $\theta_{col}^\infty = \pi/2$ if $\theta_{clean} \geqslant \pi/2$. A detailed inspection of the Reynolds number dependency reveals that as a first approximation $U_\Gamma(\theta_{clean})$ evolves between these limits as:

$$U_\Gamma(\theta_{clean}, Re) = \frac{1}{2} f^I(Re) \sin^{n(Re)}\left(\frac{\theta_{clean}}{n(Re)}\right) U_b \quad \text{for } \theta_{clean} \leqslant n(Re)\frac{\pi}{2} \tag{7}$$

$$U_\Gamma(\theta_{clean}, Re) = \frac{1}{2} f^I(Re) U_b \quad \text{for } \theta_{clean} \geqslant n(Re)\frac{\pi}{2}$$

where the coefficient n evolves between $n = 2$ for $Re = 0$ and $n = 1$ for $Re \to \infty$. A simple correlation fits the numerical values of $n(Re)$ with a difference less than 1%:

$$n(Re) = \frac{2 + 0.2Re^{0.5}}{1 + 0.2Re^{0.5}} \tag{8}$$

The curve given by (7) is reported for $Re = 10$ in Fig. 5.

The evolution of θ_{col} is reported in Fig. 6 versus θ_{clean}. For $\theta_{clean} < 90^o$ a general linear evolution is found whatever the value of the Reynolds number:

$$\theta_{col} = k(Re)\theta_{clean} \tag{9}$$

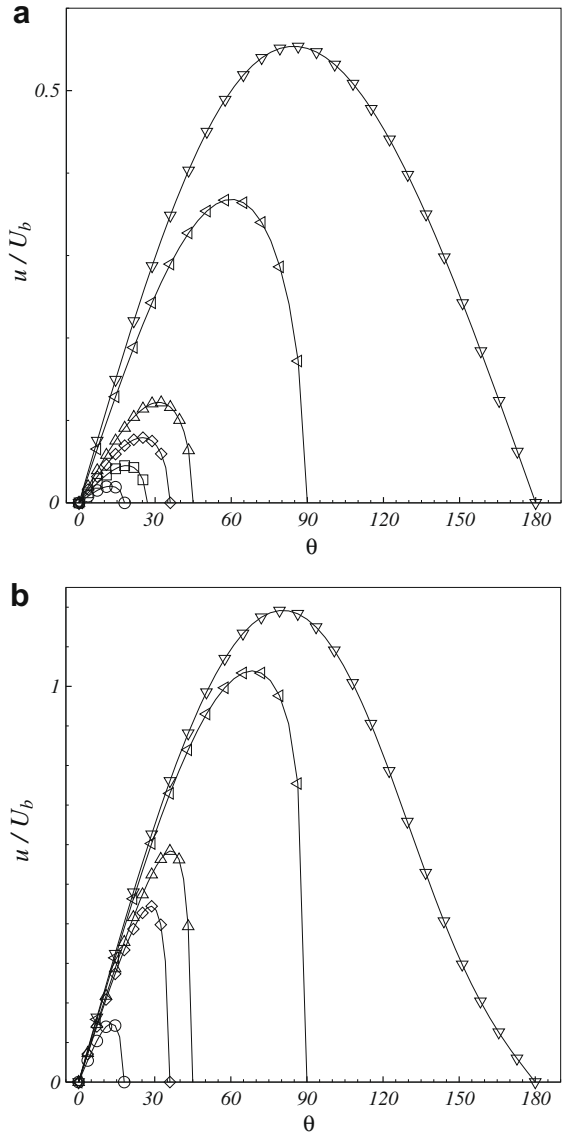

Fig. 4. Evolution of the tangential velocity $u(\theta)$ (normalized by U_b) versus θ. (a) $Re = 1$, (b) $Re = 100$. ○ $\theta_{clean} = 18°$, □ $\theta_{clean} = 27°$, ◇ $\theta_{clean} = 36°$, △ $\theta_{clean} = 45°$, ◁ $\theta_{clean} = 90°$ and ▽ $\theta_{clean} = 180°$.

where the slope $k(Re)$ depends on the Reynolds number and is found to be less than the value given by the "perfect fluid" solution $k(Re \to \infty) = 1$. The evolution of $k(Re)$ can be fit with an accuracy better than 1% with the correlation

$$k(Re) = \frac{2 + 0.16Re^{0.5}}{3 + 0.16Re^{0.5}}$$

For $\theta_{clean} > 90°$, θ_{col} tends to the value measured for a fully clean interface and is found to be nearly independent of θ_{clean} for $\theta_{clean} > 120°$. Consequently, $k(Re)$ can be estimated by $k(Re) \approx 3/4$ until $3\theta_{clean}/4$ equals the value of θ_{col} for a fully clean surface. For larger angle θ_{clean}, θ_{col} can be chosen equal to the value for a clean surface. Consequently, the probability of collision can be described using:

$$\sin(\theta_{col}) \approx \sin\left(\frac{3}{4}\theta_{clean}\right) \quad \text{for} \quad \theta_{clean} \leqslant \frac{2\pi}{3}$$
$$\sin(\theta_{col}) \approx 1 \quad \text{for} \quad \theta_{clean} \geqslant \frac{2\pi}{3} \qquad (10)$$

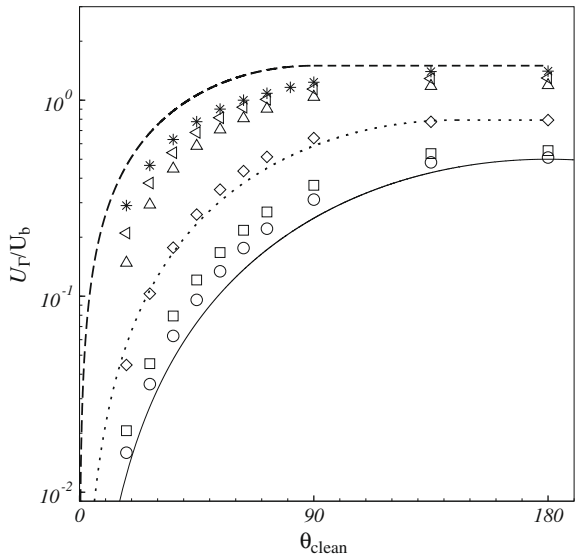

Fig. 5. Evolution of the maximum tangential velocity $U_\Gamma(\theta_{clean})$ (normalized by U_b) versus θ_{clean}. ○ $Re = 0.1$, □ $Re = 1$, ◇ $Re = 10$, △ $Re = 100$, ◁ $Re = 250$, ∗ $Re = 1000$. — $U_\Gamma^0 = 1/2\sin^2(\theta_{clean}/2)$, - - - $U_\Gamma^\infty = 3/2\sin(\theta_{clean})$, …. relation (7) for $Re = 10$.

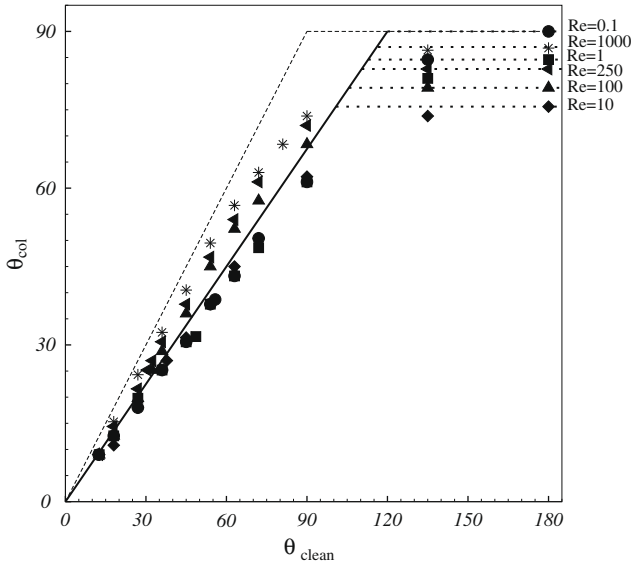

Fig. 6. Evolution of θ_{col} versus θ_{clean}. ○ $Re = 0.1$, ■ $Re = 1$, ◆ $Re = 10$, ▲ $Re = 100$, ◄ $Re = 250$, ∗ $Re = 1000$. - - - - θ_{col}^∞ (see the text), —- relation (9) with $k = 3/4$. The horizontal dotted lines represents the values of θ_{col} for a clean bubble ($\theta_{clean} = 180°$).

Finally, one propose for the probability of collision controlled by the clean part of the surface:

$$P_c\left(\frac{r_p}{r_b}, Re, \theta_{clean}\right) = \frac{r_p}{r_b}\left(1 + \frac{r_p}{r_b}\right) f^{III}(Re, \theta_{clean}) \qquad (11)$$

with

$$f^{III}(Re, \theta_{clean}) = 2\sin(\theta_{col})\frac{U_\Gamma(\theta_{clean}, Re)}{U_b} \qquad (12)$$

where $U_\Gamma(\theta_{clean}, Re)$ and $\sin(\theta_{col})$ are given by (7)–(10), respectively. This prediction is compared in Fig. 7 with numerical simulations. As observed relation (11) gives a satisfactory prediction of the effect of the interface contamination on the probability of collision with small particles in suspension when the collision is controlled by the clean part of the surface.

Note that Dukhin et al. (1995) propose to model the contamination effect by correcting the Sutherland model (i.e. for clean bubble

and $Re \gg 1$). They use the stagnant cap description for small value of θ_{clean} ($\theta_{clean} \ll \pi$). The assumption is made that the capture occurs on the front clean part of the bubble where the flow is supposed to be approximated by the potential flow. The Sutherland model is then corrected by $sin^2(\theta_{clean})$ given $f^{III}(Re \to \infty, \theta_{clean} \ll \pi) \approx 3\ sin^2(\theta_{clean})$ which is in agreement with Eq. (12) in the limit $Re \to \infty$ and $\theta_{clean} \ll \pi$. Note that for such a high level of contamination, Fig. 3 (see also Eq. 13) shows that the collision on the clean part concerns very small values of r_p/r_b since the critical ratio is then very restrictive ($(r_p/r_b)_{th} \approx \theta^3_{clean}$).

4.2. Collision controlled by the contaminated part of the surface

Fig. 8 presents the evolution of the tangential velocity gradient on the contaminated part of the interface for a partially contaminated bubble. This figure clearly shows the strong effect on the tangential velocity gradient imposed by the change of condition at the surface. After the change of surface mobility $\theta > \theta_{clean}$, the velocity gradient follows the evolution observed for a fully contaminated bubble. Two situations are observed. If $\theta_{clean} > \theta_{th}(Re)$, the velocity gradient never reaches a local maximum and the value of the flow rates can not be less than the value of the flow rate on the clean part. The probability of collision is then controlled by the clean part and evolves linearly with r_p/r_b. If $\theta_{clean} < \theta_{th}(Re)$, the velocity gradient reaches locally a maximum given by the value obtained for a fully contaminated bubble. Consequently, the flow rate of particles colliding the bubble surface is non dependent on the level of contamination and is given by relation (5). This particular behavior explains why when the flow of particles colliding the surface is controlled by the dirty part, the probability of collision is very close to the probability of a fully contaminated surface (Sarrot et al., 2005).

4.3. Estimation of the threshold value $(r_p/r_b)_{th}$

Finally, we consider the threshold value $(r_p/r_b)_{th}$ characterizing the transition between the linear and the quadratic evolution of P_c with r_p/r_b. As explained in Section 3, the transition between the two regimes is observed when the limit streamline Ψ_{col} has its two local minimum distances equal ($r_1 = r_p = r_2$). This is observed when the flow rates on the clean and the contaminated parts are equal. Since the transition is observed for $\theta_{th} < \pi/2$, Eqs. (5)–(11) gives the evolution of $(r_p/r_b)_{th}$ with the contamination:

$$\left(\frac{r_p}{r_b}\right)_{th} = \frac{f^{I}(Re)}{f^{II}(Re)} \sin^{n(Re)}\left(\frac{\theta_{clean}}{n(Re)}\right) \sin\left(\frac{3\,\theta_{clean}}{4}\right) \qquad (13)$$

In the limit $Re \to 0$, the threshold ratio is given by:

$$\left(\frac{r_p}{r_b}\right)_{th} = \frac{2}{3} \sin^2\left(\frac{\theta_{clean}}{2}\right) \sin\left(\frac{3\theta_{clean}}{4}\right)$$

Fig. 3 shows that this relation is in very good agreement with the numerical values obtained for $Re = 0.1$. For a given angle θ_{clean}, the maximum value of $(r_p/r_b)_{th}$ is approximately found for $Re \approx 20$ as confirmed by Fig. 3.

4.4. Discussion

Fig. 9 reports the evolution of the probability of collision versus r_p/r_b for different levels of contamination of the interface. This fig-

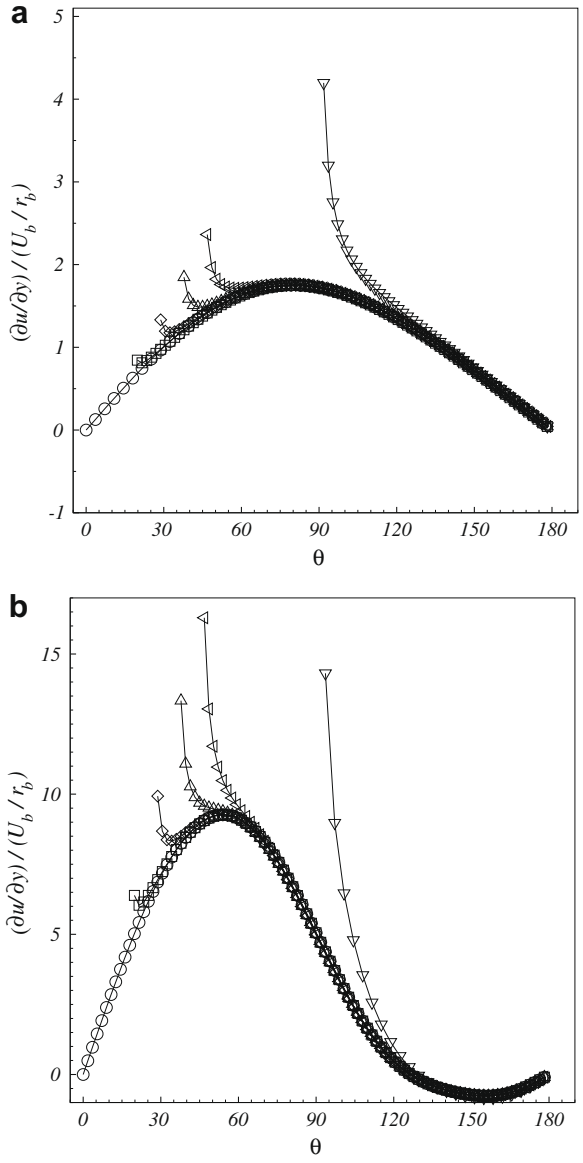

Fig. 8. Evolution of the tangential velocity gradient $\partial u/\partial y$ normalised by U_b/r_b on the contaminated part of the interface. (a) $Re = 1$, (b) $Re = 100$. ○ $\theta_{clean} = 0°$, □ $\theta_{clean} = 18°$, ◇ $\theta_{clean} = 27°$, △ $\theta_{clean} = 36°$, ◁ $\theta_{clean} = 45°$ and ▽ $\theta_{clean} = 90°$.

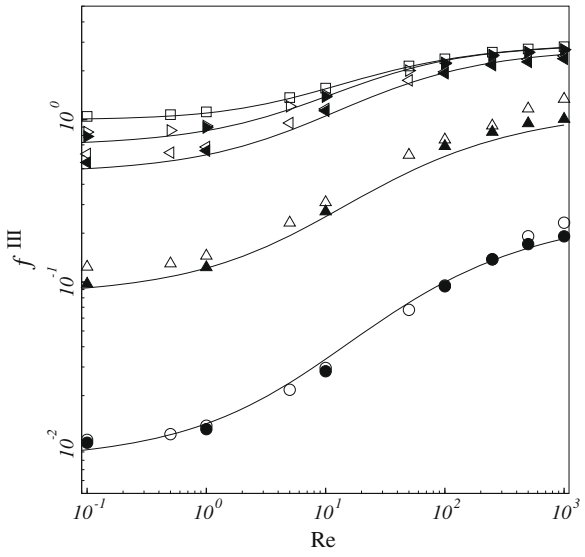

Fig. 7. Evolution of $f^{III}(Re,\theta_{clean})$ versus the Reynolds number for $r_p/r_b \leqslant (r_p/r_b)_{th}$ (Collision controlled by the clean part). Filled symbols: this study, empty symbols (Sarrot et al., 2005). ○ $\theta_{clean} = 20°$, △ $\theta_{clean} = 45°$, ◁ $\theta_{clean} = 90°$, ▷ $\theta_{clean} = 112°$, □ $\theta_{clean} = 180°$. — relation (11) for corresponding θ_{clean}.

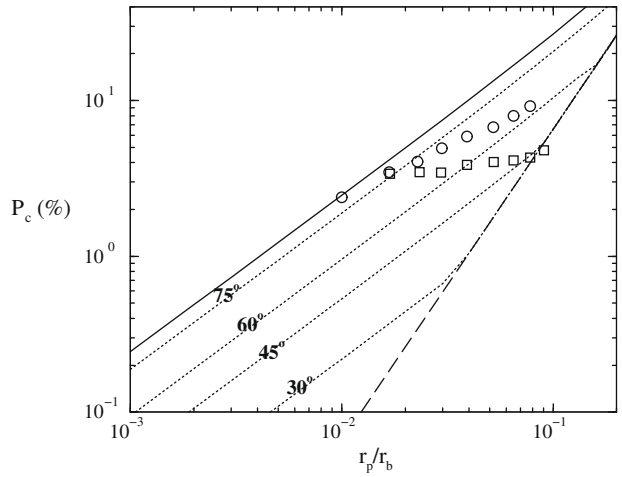

Fig. 9. Evolution of P_c versus r_p/r_b for a bubble of diameter $2r_b = 0.75$ mm in water under normal conditions. ○ Dai et al. (1997), □ Ralston et al. (2002). — $\theta_{clean} = 180°$ (Clean bubble, $U_b = 19cm/s$, $Re_b = 142$), - - - $\theta_{clean} = 0°$ (Fully contaminated bubble, $U_b = 8{,}5cm/s$, $Re_b = 64$), ... $\theta_{clean} = 30°$ ($U_b = 8.5cm/s$, $Re_b = 64$), $45°$ ($U_b = 8.6cm/s$, $Re_b = 64$), $60°$ ($U_b = 8.7cm/s$, $Re_b = 65$) and $75°$ ($U_b = 9cm/s$, $Re_b = 68$).

ure illustrates the strong influence of the contamination specially for high level of contamination. The bubble radius is $2r_b = 0.75$ mm to make possible the comparison with some experiments available in the literature. A presentation on the different experimental approaches is reported in Nguyen and Schulze (2004). Experimental determination of collision probability is very delicate and it is very difficult to experimentally distinguish the collision efficiency from the other efficiencies (attachment and stability of the aggregate). To simplify the number of effect involved in the capture, experimental determinations of the bubble-particle encounter efficiency are usually carried out with simplified systems. These experiments concerns single bubbles in a well-defined hydrodynamic flow field and strongly hydrophilic or strongly hydrophobic particles. In the latter case, the efficiency of attachment approximately equals unity and the collision efficiency equals the experimental collection efficiency if fine particles are used. The particle capture probability per bubble is measured by injecting single bubbles in a suspension of particles (Hewitt et al., 1994; Dai et al., 1998; Ralston et al., 2002; Sarrot et al., 2007). The water quality is also controlled in order to avoid the bubble contamination and electrostatic interaction are suppressed by introducing an appropriate concentration of KCl. Consequently, only experiments for clean bubble are available in the literature. Some of these experiments are reported on Fig. 9 for spherical bubbles of radius closed to $2\,r_b = 0.75$ mm. For all the experiments reported the rising velocity is found to be close to $20cm/s$ indicating a fully mobile interface. We have reported the data obtained by Dai et al. (1997) for a very dilute pulp of hydrophobized quartz particles ($7\ \mu m \leqslant d_p \leqslant 70\ \mu m$) corresponding to Stokes number $0.002 \leqslant St \leqslant 0.14$. The experimental results tends to the evolution of a clean bubble in the limit of small Stokes numbers (i.e. small r_p/r_b). For larger Stokes numbers a significant deviation is observed due to the particle inertia (Nguyen, 1998). The same tendency is observed for experiments reported in Ralston et al. (2002) with quartz particles in the same range of radius and with a contact angle of 73°. Note that Ralston et al. (2002) also analyze the effect of the particle hydrophobicity which is shown to significantly modifies the collection efficiency (we have reported here the results obtained with the stronger hydrophobicity). Fig. 9 clearly shows that the effect induced by a partially contaminated surface is of the same order of magnitude than the effect of inertia and hydrophobicity of the particles in suspension. Finally, some additional experiments controlling the bubble contamination are necessary in order to evaluate the relative effects of the bubble contamination, the particle inertia and the particle hydrophobicity.

5. Conclusion

In this paper, the probability of collision of a spherical bubble moving in a suspension of fine particles has been evaluated up to order $(r_p/r_b)^2$. The dependency with the Reynolds number and the level of contamination of the interface has also been investigated. The collision efficiency is expressed as $P_c(r_p/r_b, Re) = g(r_p/r_b)\ f(Re)$ for both mobile and immobile interface. For a clean bubble, $g(r_p/r_b) = r_p/r_b(1 + r_p/r_b)$ while for a fully contaminated bubble (or a solid sphere) $g(r_p/r_b) = (r_p/r_b)^2$. These behaviors are given by the flux of particles near the surface which is controlled by the tangential velocity for mobile interfaces and by the velocity gradient for immobile interfaces. For a clean bubble $f(Re)$ is a monotonic function evolving from *1* for Stokes flow to *3* for high Reynolds number. For a fully contaminated bubble (or solid sphere) the collision efficiency reaches the Stokes limit $f(Re) = 3/2$ at low Reynolds number while it evolves as $Re^{1/2}$ at high Reynolds number. One direct consequence is that the probability of collision with a contaminated bubble is much smaller that for a clean bubble when $r_p \ll r_b$. For a partially contaminated bubble a linear or a quadratic dependency in r_p/r_b is found depending on the level of contamination and the value of r_p/r_b. The transition between the r_p/r_b and $(r_p/r_b)^2$ dependency is observed at a threshold value $(r_p/r_b)_{th}$ evolving as $\sin^{n(Re)}(\theta_{clean}/n(Re))\sin(3\theta_{clean}/4)$ where $n(Re)$ is a coefficient varying from $n(0) = 2$ to $n(\infty) = 1$ from small to large Reynolds numbers. If θ_{clean} is less than a transition angle θ_{th} and the radii ratio is larger than $(r_p/r_b)_{th}$, then the probability of collision is that of a fully contaminated bubble and evolves as $(r_p/r_b)^2$. For all the other situations the probability of collision evolves linearly with r_p/r_b and is proportional to $\sin^{n(Re)}(\theta_{clean}/n(Re))\ \sin(3\theta_{clean}/4)$ when $\theta_{clean} < \pi/2$ while it is close to the probability obtained for a clean bubble for $\theta_{clean} > \pi/2$.

References

Bel, F.R., Duineveld, P., 1996. The effect of surfactant on the rise of a spherical bubble at high reynolds and peclet numbers. Phys. Fluids A 8 (2), 310–321.

Clift, R., Grace, J.R., Weber, M.E., 1978. Bubbles. Drops and Particules. Academic Press, New York.

Cuenot, B., Magnaudet, J., Spennato, B., 1997. The effect of slightly soluble surfactant on the flow around a spherical bubble. J. Fluid Mech. 339, 25–53.

Dai, Z., Dukhin, S., Fornasiero, D., Ralston, J., 1997. The inertial hydrodynamic interaction of particles and rising bubbles with mobile surfaces. J. Colloid interface Sci. 197, 275–292.

Dai, Z., Dukhin, S., Fornasiero, D., Ralston, J., 1998. The inertial hydrodynamic interaction of particles and rising bubble with mobile surfaces. J. Colloid Interface Sci. 197, 275–292.

Dai, Z., Fornasiero, D., Ralston, J., 2000. Particle-bubble collision models – a review. J. Colloid Interface Sci. 85, 231–256.

Dukhin, S.S., Kretzchmar, G., Miller, B., 1995. Dynamics of Adsorption at Liquid Interfaces. Elsevier, Amsterdam.

Gaudin, A.M., 1957. Flotation. Second ed. McGraw-Hill, New York.

Hewitt, D., Fornasiero, D., Ralston, J., 1994. Bubble particle attachment efficiency. Miner. Eng. 7, 657–665.

Legendre, D., 2007. On the relation between the drag and the vorticity produced on a clean bubble. Phys. Fluids 19, 018102.

McLaughlin, J.B., 1996. Numerical simulation of bubble motion in water. J. Colloid Interface Sci. 184, 614–625.

Moore, D.W., 1963. The boundary layer on a spherical gas bubble. J. Fluid Mech. 16, 161–176.

Nguyen, A.V., 1998. Particle-bubble encounter probability with mobile bubble surface. Int. J. Miner. Process. 55, 73–86.

Nguyen, A.V., Ralston, J., Schulze, H.J., 1998. On modelling of bubble-particle attachment probability in flotation. Int. J. Miner. Process. 53, 225–249.

Nguyen, A.V., Schulze, H.J., 2004. Colloidal Science of Flotation. Surfactant Sciences Series, 118. Marcel Dekker, Inc., New York.

Ralston, J., Dukhin, S.S., Mishchuk, N.A., 2002. Wetting film stability and flotation kinetics. Adv. Colloid Interface Sci. 95, 145–236.

Sadhal, S.S., Johnson, R.E., 1983. Stokes flow past bubbles and drop partially coated with thin films. J. Fluid Mech. 126, 237.

Sarrot, V., 2006. Capture de fines particules par des inclusions fluides. Institut National des Sciences Appliquées de Toulouse, Toulouse, France..
Sarrot, V., Guiraud, P., Legendre, D., 2005. Determination of the collision frequency between bubbles and particles in flotation. Chem. Eng. Sci. 60 (22), 6107–6117.
Sarrot, V., Huang, Z., Legendre, D., Guiraud, P., 2007. Experimental determination of particles capture efficiency in flotation. Chem. Eng. Sci. 62, 7359–7369.
Schulze, H., 1989. Rate of capture of small particles in flotation. Mineral Processing and Extractive Metallurgy Review 5, 43–76.
Sutherland, K.L., 1948. Physical chemistry of flotation xi. Kinetics of the flotation process. J. Phys. Chem. 52, 394–425.
Weber, M.E., Paddock, D., 1983. Interceptional and gravitational collision efficiencies for single collectors at intermediate reynolds number. J. Colloid Interface Sci. 94 (2), 328–335.
Yoon, R.H., Lutrell, G.H., 1989. The effect of bubble size on fine particle flotation. Min. Process. Extractive Metall. Rev. 5, 101–122.